ROBUST FUZZY-PID CONTROL OF THREE-MOTOR DRIVE SYSTEM USING SIMULATED ANNEALING OPTIMIZATION

Fawzan SALEM **E.H.E. BAYOUMI**
Power Electronics and Energy Conversion Department,
Electronics Research Institute (ERI),
Cairo, Egypt
E-mail: fawzan@lycos.com

Abstract: *Multi-motor drive system is a multi-input multi-output (MIMO), nonlinear and strong-coupling system. In turn to improve synchronous performance of multi-motor system, this paper presents a synchronous control system for three-induction motors. It includes three robust Fuzzy-PID controllers based Simulated Annealing Optimization (SAO). The parameters of Fuzzy-PID controllers are adjusted for fulfilling the open loop control of multi-variable system to reduce mutual coupling effect. The SAO technique is used to adjust the input and output scaling factor (SF's) by minimizing both integral of absolute of errors (IAE) and integral of time multiplied absolute of errors (ITAE) as performance measures. To test the robustness of the proposed system, several sudden changes are presented. The results indicate that the control system can acquire the optimal parameters of the Fuzzy-PID controllers according to different running states of the system. Results of system performance endorse the proposed technique and emphasize its feasibility.*

Keywords: *three-motor drive system, Fuzzy-PID controllers, Simulated Annealing Optimization.*

1. Introduction

Due to its high precision coordinated control performance, a multi-motor system has attracted more and more attentions in the drive applications such as urban rail transit, paper making, electric vehicle drive, and steel rolling [1-5]. The AC multi-motor drive system is a multi-input multi-output (MIMO), nonlinear and strong-coupling system [6, 7]. Thus, its accurate mathematical model is hard to obtain. Meanwhile, industrial production also requires the multi-motor drive control system to decouple the speed and tension, which increases the control difficulty.

Nowadays, common decoupling control methods mainly contain: improved control algorithm based on the traditional PID [8], cross-coupled control [9], feed forward control [10], optimal control [11], sliding mode control [12, 13], BP Neural Network [14], and fuzzy control [15]. To a certain degree, these methods have improved coordinated control performance. However, it should be noted that most of the existing methods depend on dynamic model of the motor and traditional single motor drive system.

Fuzzy-PID control, as one of the promising intelligent control techniques, is applied for multi-motor synchronous control purposes. The authors in [16] proposed a variable gain intelligent Fuzzy reasoning control scheme in the stretch tension and synchronization control system of a wide-fabric heating-shaping machine. In [17] a synchronization control strategy of multi-motor system based on PROFIBUS network was proposed using BP Neural Network and an adaptive double mode Fuzzy-PID arithmetic. Fuzzy-PID C-means clustering algorithm [18] was applied to two-motor variable frequency speed-regulating synchronous system as a multivariable nonlinear coupling system. It is used to cluster the data of input-output according to a satisfactory performance index in order to identify speed and tension for the two-motor synchronous system based on local model networks. Two different Fuzzy-PID decoupling controllers in the speed feedback and the tension feedback [19] introduced greatly improved performance. It should be noted that most of these researches consider only two-motor synchronous drive system.

There are several researches in the literature employed Simulated Annealing Optimization (SAO) in Fuzzy-PID controllers. The authors in [20] proposed a general technique for optimizing fuzzy models in fuzzy expert systems (FES's) by simulated annealing (SA) and N-dimensional simplex method. In [21], Fuzzy-PID control is combined with BP Neural Network with a Genetic Algorithms (GA) and SAO to short-term load forecasting. An optimizing

Fuzzy Neural Networks for tuning PID controllers using an SAO was proposed, in [22], to solve the large-scale constrained optimization problems. The authors in [23] discuss the design of fuzzy control systems with a reduced parametric sensitivity using simulated-annealing algorithms.

This paper introduces a robust Fuzzy-PID control of three-motor drive system using SAO. The main objective is to minimize both the integral of absolute of errors (IAE) and the integral of time multiplied absolute of errors (ITAE) as performance measures. SAO technique is applied to adjust the parameters of Fuzzy-PID controllers for reducing the strong coupling influences. The rest of the paper is organized as follows; section 2 formulates the mathematical model of the three-motor drive system by considering the first motor as a main and the others as supplement motors. In section 3, the proposed Fuzzy-PID controller is applied to the three-motor system. Moreover, the SAO algorithm is presented to optimize the input and output scaling factor (SF's) such that the overall performance index is minimized. Different simulation cases are studied and presented in section 4. The proposed system robustness is tested by applying several sudden changes. The results are compared with those obtained using PID controllers whose gains are optimized also by SAO to guarantee fair comparison. Conclusions, remarks and perspectives of applying the proposed Fuzzy-PID controller to multi-motor drive system are discussed in section 5.

2. Mathematical Model

Figure 1 shows the block diagram of three-induction motor drive system, in which motor 1 is the main motor and other two motors are supplement motors. Every motor and its inverter can be regarded as a modular cell. The belt-pulley is installed on the motor shaft, and motors are combined by transmission belt on the belt-pulley. When the motors run, the rotation of their rotors pulls the belt to operate coordinately.

According to Hooke law and by considering the amount of forward slip, the tensions between the two adjacent motors can be expressed as:

$$\dot{F}_{12} = \frac{K_1}{T_1}\left(\frac{r_1 a_1}{p_1}\omega_{r1} - \frac{r_2 a_2}{p_2}\omega_{r2}\right) - \frac{F_{12}}{T_1} \quad (1)$$

$$\dot{F}_{12} = \frac{K_2}{T_2}\left(\frac{r_2 a_2}{p_2}\omega_{r2} - \frac{r_3 a_3}{p_3}\omega_{r3}\right) - \frac{F_{23}}{T_2} \quad (2)$$

where:

F_{12}, F_{23}	tensions of the belt;
$K_1=E/V_1$, $K_2=E/V_2$	transfer coefficients;
$T_1=L_1/(AV_1)$, $T_2=L_2/(AV_2)$	time constants of tension variation;
r_i	radius of i belt-pulley (i =1,2,3);
a_i	number i speed ratio;
ω_{ri}	electric angular speed of i motor,
p_i	pole-pairs number of i motor;
A	sectional area of the belt;
E	Young's Modulus of the belt;
L_1, L_2	distances between the two motors;
V_1, V_2	line speed.

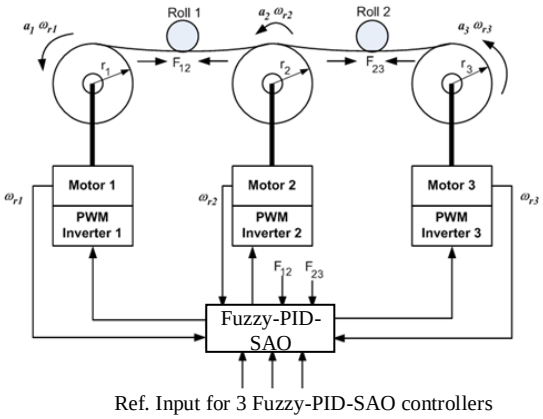

Fig. 1. The three-motor drive system.

The three-motor model can be expressed by:

$$\dot{\omega}_{r1} = \frac{p_1}{J_1}\left[(\omega_1 - \omega_{r1})\frac{p_1\tau_{r1}}{L_{r1}}\phi_{r1}^2 - (T_{L1} + r_1 F_{12})\right]$$

$$\dot{\phi}_{r1} = \frac{L_{m1}}{\tau_{r1}} i_{sd1} - \frac{1}{\tau_{r1}}\phi_{r1}$$

$$\dot{\omega}_{r2} = \frac{p_2}{J_2}\left[(\omega_2 - \omega_{r2})\frac{p_2\tau_{r2}}{L_{r2}}\phi_{r2}^2 - (T_{L2} - r_2 F_{12} + r_2 F_{23})\right]$$

$$\dot{\phi}_{r2} = \frac{L_{m2}}{\tau_{r2}} i_{sd2} - \frac{1}{\tau_{r2}}\phi_{r2} \quad (3)$$

$$\dot{\omega}_{r3} = \frac{p_3}{J_3}\left[(\omega_3 - \omega_{r3})\frac{p_3\tau_{r3}}{L_{r3}}\phi_{r3}^2 - (T_{L3} - r_3 F_{23})\right]$$

$$\dot{\phi}_{r3} = \frac{L_{m3}}{\tau_{r3}} i_{sd3} - \frac{1}{\tau_{r3}}\phi_{r3}$$

In vector control technique, the rotor flux is kept constant. Then the three-motor model can be reduced to:

$$\dot{\omega}_{r1} = \frac{p_1}{J_1}[(\omega_1 - \omega_{r1})\frac{p_1\tau_{r1}}{L_{r1}}\phi_{r1}^2 - (T_{L1} + r_1F_{12})]$$

$$\dot{\omega}_{r2} = \frac{p_2}{J_2}[(\omega_2 - \omega_{r2})\frac{p_2\tau_{r2}}{L_{r2}}\phi_{r2}^2 - (T_{L2} - r_2F_{12} + r_2F_{23})]$$

$$\dot{\omega}_{r3} = \frac{p_3}{J_3}[(\omega_3 - \omega_{r3})\frac{p_3\tau_{r3}}{L_{r3}}\phi_{r3}^2 - (T_{L3} - r_3F_{23})] \quad (4)$$

The mathematical model for the whole drive system is represented by:

$$\dot{\omega}_{r1} = \frac{p_1}{J_1}[(\omega_1 - \omega_{r1})\frac{p_1\tau_{r1}}{L_{r1}}\phi_{r1}^2 - (T_{L1} + r_1F_{12})]$$

$$\dot{\omega}_{r2} = \frac{p_2}{J_2}[(\omega_2 - \omega_{r2})\frac{p_2\tau_{r2}}{L_{r2}}\phi_{r2}^2 - (T_{L2} - r_2F_{12} + r_2F_{23})]$$

$$\dot{\omega}_{r3} = \frac{p_3}{J_3}[(\omega_3 - \omega_{r3})\frac{p_3\tau_{r3}}{L_{r3}}\phi_{r3}^2 - (T_{L3} - r_3F_{23})]$$

$$\dot{F}_{12} = \frac{K_1}{T_1}(\frac{r_1a_1}{p_1}\omega_{r1} - \frac{r_2a_2}{p_2}\omega_{r2}) - \frac{F_{12}}{T_1}$$

$$\dot{F}_{12} = \frac{K_2}{T_2}(\frac{r_2a_2}{p_2}\omega_{r2} - \frac{r_3a_3}{p_3}\omega_{r3}) - \frac{F_{23}}{T_2} \quad (5)$$

where

J_1, J_2, J_3 rotor inertia;

τ_{r1}, τ_{r2}, τ_{r3} electromagnetic time constant;

T_{L1},T_{L2}, T_{L3} load torque;

Φ_{r1}, Φ_{r2}, Φ_{r2} rotor flux;

L_{r1},L_{r2}, L_{r3} rotor self-inductance;

i_{sd1}, i_{sd2}, i_{sd3} *d*-axis stator current;

ω_1, ω_2, ω_3 synchronous angular speed of stator's.

From equation (5), we can find the result of coupling are existing between the speeds of the three motors, the tension F_{12} and the tension F_{23}, they are strongly coupled.

Solving equation (5) by using Laplace transform,

$$\Omega_{r1}(s) = \frac{1}{s+\beta_1}\left[\beta_1\omega_1 - \frac{p_1}{J_1}(T_{L1}(s) + r_1F_{12}(s))\right]$$

$$\Omega_{r2}(s) = \frac{1}{s+\beta_2}[\beta_2\omega_2 - \frac{p_2}{J_2}(T_{L2}(s) - r_2(F_{12}(s) + F_{23}(s)))]$$

$$\Omega_{r3}(s) = \frac{1}{s+\beta_3}\left[\beta_3\omega_3 - \frac{p_3}{J_3}(T_{L3}(s) - r_3F_{23}(s))\right]$$

$$F_{12}(s) = \frac{K_1}{(T_1s+1)}\left[\frac{r_1a_1}{p_1}\Omega_{r1}(s) - \frac{r_2a_2}{p_2}\Omega_{r2}(s)\right] \quad (6)$$

$$F_{23}(s) = \frac{K_2}{(T_2s+1)}\left[\frac{r_2a_2}{p_2}\Omega_{r2}(s) - \frac{r_3a_3}{p_3}\Omega_{r3}(s)\right]$$

where,

$$\beta_1 = \frac{p_1^2\tau_{r1}}{J_1L_{r1}}\phi_{r1}^2, \quad \beta_2 = \frac{p_2^2\tau_{r2}}{J_2L_{r2}}\phi_{r2}^2,$$

and $\beta_3 = \frac{p_3^2\tau_{r3}}{J_3L_{r3}}\phi_{r3}^2$ (7)

Figure (2.a) shows a Matlab/Simulink model of the equations (1-3) for the three-motor system, while figure (2.b) shows a Matlab/Simulink model of the equations (4-5) for the same system.

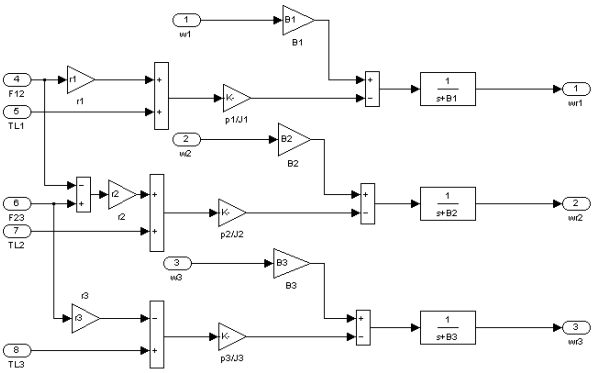

Fig. 2. Simulink three-motor model equations. (1-3).

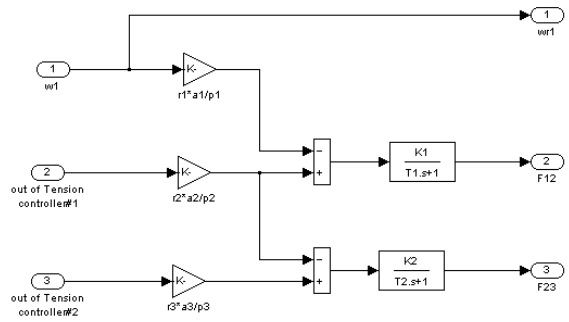

Fig. 3. Simulink three-motor model equations. (4-5).

3. The Proposed System Design Tools

3.1 Controllers Design for Speed/Tension Loops

A Fuzzy-PID-SAO controller is proposed to improve the synchronous performance of three AC induction motors control system. Three different Fuzzy-PID-SAO controllers are designed, one for the speed and two for the tensions. In the proposed approach, the gains of a PID controller are primary guessed using Ziegler-Nichols approach, and then these gains are utilized to get the corresponding values for input and output scaling factors of the proposed Fuzzy-PID-SAO controller. These values are employed to suggest the ranges of the Fuzzy-PID-SAO tuning parameters (input and output SF's) for the SAO algorithm. The optimization algorithm is then applied to obtain the best values for the input and output SF's of the Fuzzy-PID-SAO controllers. Fig. (4) shows a schematic diagram for the overall control system while Fig. (5) shows the Fuzzy-PID-SAO controller structure for the speed loop. The Fuzzy-PID-SAO controllers for both tension loops are the same except for their input and output SF's.

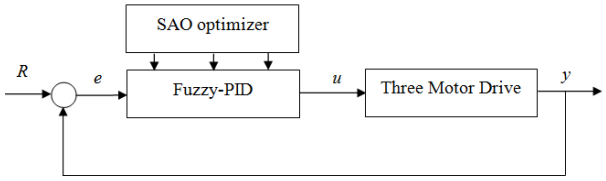

Fig. 4. A diagram for the overall control system

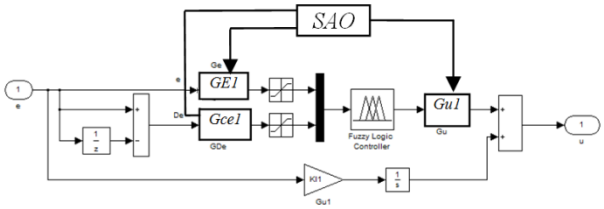

Fig. 5. Simulink for speed Fuzzy-PID-SAO

3.1.1 Membership Functions

All membership functions (MF's) controller inputs, i.e. error (e) and change of error (Δe) and controller output for Fuzzy-PID-SAO (u) are defined on the normalized interval [1, 1] since the arbitrary selection of the universe of discourse causes some complexity in the selection of the scaling factors. We use five symmetric triangles membership functions with 50% overlapping with neighboring for both error and change of error for the three Fuzzy-PID-SAO controllers. Five singletons output membership functions are applied for the control signal. The input and output MF's are shown in Fig. 6.

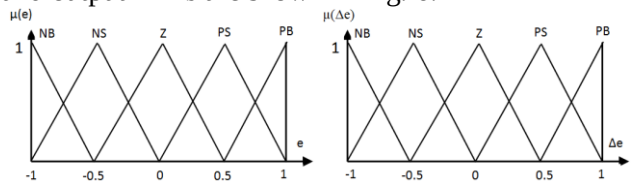

Fig. 6.a. Input MF's for the error and change of error

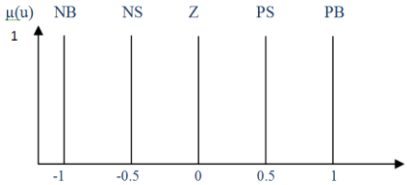

Fig. 6.b. Output MF's for the control signal

Fig. 6. Input and Output membership functions

3.1.2 Rule Base

Rule tables for Fuzzy-PID-SAO controllers are obtained from the analysis of the system behavior. The Fuzzy-PID-SAO controller works in such a way that relates the controlled system output with the reference input by a set of fuzzy rules. These rules are the most important part of the controller structure and they must be obtained correctly so that the relationship between input and output of the controlled system are represented properly. The set of fuzzy rules should be determined and organized in such a way that the reference set point is tracked with the best performance measures. These performance measures are; minimum overshoot, rise time, settling time, integral of absolute of errors, and integral of time multiplied absolute of errors. Table (1) shows the applied fuzzy rule base.

Table (1). The Fuzzy rule base utilized for the proposed Fuzzy-PID-SAO controller

e \ Δe	NB	NS	Z	PS	PB
NB	NB	NB	NS	NS	Z
NS	NB	NS	NS	Z	PS
Z	NS	NS	Z	PS	PS
PS	NS	Z	PS	PS	PB
PB	Z	PS	PS	PB	PB

In this work, we select the fuzzy implication as product-max, where the algebraic product is utilized for AND-connective while the rule base is the outer AND-product of all input families. Center of area method is applied for the defuzzification process.

3.2 Simulated Annealing Optimization

Annealing is the process of heating the solid body to a high temperature and allowed it to cool slowly. Annealing causes the particles of the solid material to reach the minimum energy state. This is due to the fact that when the solid body is heated to the very high temperature, the particles of the solid body are allowed to move freely and when it is cooled slowly, the particles are able to arrange themselves so that the energy of the particles are made minimum. The mathematical equivalence of the thermodynamic annealing as described above is called simulated annealing [24].

The energy of the particle in thermodynamic annealing process is corresponding to the cost function to be minimized in optimization problems. Similarly, there is an analogy between the particles of the solid and the independent variables used in the minimization function. Initially the values assigned to the variables are randomly selected from a wide range of values. The cost function corresponding to the selected values are treated as the energy of the current state. Searching the values from the wide range of the values can be compared with the particles flowing in the solid body when it is kept in high temperature.

The next energy state of the particles is obtained when the solid body is slowly cooled. This is equivalent to randomly selecting next set of the values. When the solid body is slowly cooled, the particles of the body try to reach the lower energy state. But as the temperature is high, random flow of the particles still continues and hence there may be chance for the particles to reach higher energy state during this transition. Probability of reaching the higher energy state is inversely proportional to the temperature of the solid body at that instant. The values are randomly selected so that cost function of the currently selected random values is minimum compared with the previous cost function value. At the same time, the values corresponding to the higher cost function compared with the previous cost function are also selected with some probability. The probability depends upon the current simulated temperature 'T'. If the temperature is large, probability of selecting the values corresponding to higher energy levels are more. This process of selecting the values randomly is repeated for a finite number of iterations. The values obtained after the finite number of iterations can be assumed as the values with lowest energy state.

Most studies have applied a single-error criterion for representing overall performance. However, it is difficult to conduct a performance assessment for optimal control based on response error signals due to the conflicting requirements between static and dynamic responses and which may lead to a poor design with respect to other performance indexes.

In this work, both integral of absolute of errors (IAE) and integral-of-time-multiplied absolute of errors (ITAE) are taken as individual indexes to cover both static and dynamic responses. IAE and ITAE reflect the transient and steady-state characteristics of the control system, respectively. They have a significant insight about the system response because the mere observations of response curves are not sufficient to evaluate the control system performance. It is noted that large errors lead to large values for IAE, while ITAE penalizes heavily errors that occur late in time.

The optimization problem is to estimate the best values for the input scaling factors ('G_e' and '$G_{\Delta e}$') as well as the output scaling factor (G_u) of the Fuzzy-PID-SAO controllers such that the cost function $f(G_e, G_{\Delta e}, G_u)$ is minimized where 'G_e' varies from 'G_e min' to 'G_e max', '$G_{\Delta e}$' varies from '$G_{\Delta e}$ min' to '$G_{\Delta e}$ max', and 'G_u' varies from 'G_u min' to 'G_u max'. Suppose J_T is the overall performance index of the system.

$$J_T = f(G_{ec}, G_{\Delta ec}, G_{uc}) = w1 \text{ X IAE} + w2 \text{ X ITAE} \quad (8)$$

Where w1 and w2 are weighting factors used in the case that indexes have large difference in their magnitudes; and it can also emphasize some specific performance indexes over others. It should be noted that the smaller the value of J_T, the better the performance.

Thus, the SAO can be summarized as follow:

Step 1: Initialize the value of the temperature 'T'.

Step 2: Randomly select the current values for the variables 'G_e', '$G_{\Delta e}$' and 'G_u' from their allowable ranges. Let them be 'G_{ec}', '$G_{\Delta ec}$' and 'G_{uc}', respectively.

Step 3: Compute the corresponding cost function value $f(G_{ec}, G_{\Delta ec}, G_{uc})$.

Step 4: Randomly select the next set of values for the variables 'G_e', '$G_{\Delta e}$' and 'G_u' from their allowable ranges. Let them be 'G_{en}', '$G_{\Delta en}$' and 'G_{un}' respectively.

Step 5: Compute the corresponding cost function value $f(G_{en}, G_{\Delta en}, G_{un})$.

Step 6: If $f(G_{en}, G_{\Delta en}, G_{un}) <= f(G_{ec}, G_{\Delta ec}, G_{uc})$, then the current values for the random variables $G_{ec} = G_{en}$, $G_{\Delta ec} = G_{\Delta en}$ and $G_{uc} = G_{un}$.

Step 7: If $f(G_{en}, G_{\Delta en}, G_{un}) > f(G_{ec}, G_{\Delta ec}, G_{uc})$, then the current values for the random variables $G_{ec} = G_{en}$, $G_{\Delta ec} = G_{\Delta en}$ and $G_{uc} = G_{un}$ are assigned when

$$exp\,[(f(G_{ec}, G_{\Delta ec}, G_{uc}) - f(G_{en}, G_{\Delta en}, G_{un})) / T] > rand$$

Note that when the temperature 'T' is less, the probability of selecting the new values as the current values is less.

Step 8: Reduce the temperature T = r X T, where r is a scaling factor varying from 0 to 1.

Step 9: Repeat STEP 3 to STEP 8 for n times until 'T' reduces to the particular percentage of initial value assigned to 'T'.

4. Results

Both PID-SAO and Fuzzy-PID-SAO controllers are applied to the three-induction motors drive system. The SAO algorithm given in this paper is achieved by using Matlab software. Figures (4) and (5) show how SAO optimizer is utilized on-line to adjust the controllers tuning parameters. The SAO, on-line, optimizes the controller parameters of both the PID-SAO controllers (k_p, T_d, and T_i) as well as the Fuzzy-PID-SAO controllers (input and output SF's) to enhance the controller response. Hence, the maximum degree of system stability is obtained by

solving the minimize optimization problem via SAO. Ziegler-Nichols tuning method is utilized as an initial guess for the PID controller parameters.

In order to show the validity of the proposed Fuzzy-PID-SAO controllers, the performances of the proposed controllers are compared to the performances of the PID-SAO controllers in terms of integral absolute error (IAE) and integral time-multiplied absolute error (ITAE). To test the robustness of the proposed system, several simulation cases are considered to evaluate the performance of both PID-SAO and Fuzzy-PID-SAO controllers.

Case (1): A step sudden increase in speed reference from 300 to 500 r/min at the tenth second is given in Fig. 7-a. The speed Fuzzy-PID-SAO controller shows a faster response and better measure for IAE and ITAE compared to PID-SAO controller. In the other hand, the two-tension Fuzzy-PID-SAO controllers for F12 and F23 give robust and faster responses compared to PID-SAO controllers as shown in Fig. 7(b-c). Referring to the results shown in table (2), IAE measures for speed and tensions F12 and F23 Fuzzy-PID-SAO controllers have been reduced by 45.9%, 44.38% and 44.6%, respectively compared to PID-SAO controller. ITAE measures for speed and tensions F_{12} and F_{23} Fuzzy-PID-SAO controllers have been reduced by 47.21%, 44.3% and 44%, respectively compared to SAO-PID controller.

Case (2): A step sudden decrease in speed reference from 500 to 300 r/min at the tenth second is given in Fig. 8-a. Again, the speed and tension Fuzzy-PID-SAO controllers show faster responses and give better measures for IAE and ITAE compared to PID-SAO controller as shown in Figures 8(b-c). Table (2) shows that IAE measures for speed and tensions F12 and F23 Fuzzy-PID-SAO controllers have been reduced by 45.9%, 44.84% and 44.53%, respectively compared to PID-SAO controller. Moreover, ITAE measures for speed and two tensions Fuzzy-PID-SAO controllers have been reduced by 47.69%, 44.7% and 44.64%, respectively compared to SAO-PID controller.

Case (3): A step sudden change in tension F_{12} reference from 20 to 25 r/min at the tenth second is given in Fig. 9-a. The speed and two tensions Fuzzy-PID-SAO controllers show faster responses and give enhanced measures for IAE and ITAE compared to PID-SAO controller as shown in Figures 9(b-c). Table (2) shows that IAE measures for speed and tensions F12 and F23 Fuzzy-PID-SAO controllers have been reduced by 45.88%, 44.5% and 44.4%, respectively compared to PID-SAO controller. In addition, ITAE measures for speed and two tensions Fuzzy-PID-SAO controllers have been reduced by 72.8%, 44.5% and 44.4%, respectively compared to SAO-PID controller.

Case (4): A step sudden decrease in tension F_{23} reference from 30 to 25 r/min at the tenth second is given in Fig. 10-a. The speed and tension Fuzzy-PID-SAO controllers show faster responses and better measure for IAE and ITAE compared to PID-SAO controller as shown in Figures 10(b-c). Table (2) shows that IAE measures for speed and tensions F12 and F23 Fuzzy-PID-SAO controllers have been reduced by 45.88%, 40.53% and 36.64%, respectively compared to PID-SAO controller. Also, the ITAE measures for speed and tensions F_{12} and F_{23} Fuzzy-PID-SAO controllers have been reduced by 72.76%, 40.69% and 36.23%, respectively compared to SAO-PID controller.

Table 2. Comparison between the response of both PID-SAO and Fuzzy-PID-SAO controllers

Case	Controller	IAE	ITAE	Response
First Case	PID-SAO	108.9	458	Speed
	Fuzzy-PID-SAO	58.93	241.8	
	PID-SAO	3.38	2.98	F_{12}
	Fuzzy-PID-SAO	1.88	1.66	
	PID-SAO	4.82	3.25	F_{23}
	Fuzzy-PID-SAO	2.67	1.85	
Second Case	PID-SAO	152.5	466.9	Speed
	Fuzzy-PID-SAO	82.5	244.2	
	PID-SAO	3.59	3.18	F_{12}
	Fuzzy-PID-SAO	1.98	1.76	
	PID-SAO	5.03	3.45	F_{23}
	Fuzzy-PID-SAO	2.79	1.91	
Third Case	PID-SAO	108.9	22.27	Speed
	Fuzzy-PID-SAO	58.93	6.06	
	PID-SAO	4.09	8.13	F_{12}
	Fuzzy-PID-SAO	2.27	4.51	
	PID-SAO	4.82	3.29	F_{23}
	Fuzzy-PID-SAO	2.68	1.83	
Fourth Case	PID-SAO	108.9	22.26	Speed
	Fuzzy-PID-SAO	58.93	6.06	
	PID-SAO	3.38	2.31	F_{12}
	Fuzzy-PID-SAO	2.01	1.37	
	PID-SAO	5.54	8.39	F_{23}
	Fuzzy-PID-SAO	3.51	5.35	
	Fuzzy-PID-SAO	2.91	4.39	
	Fuzzy-PID-SAO	3.32	9.98	

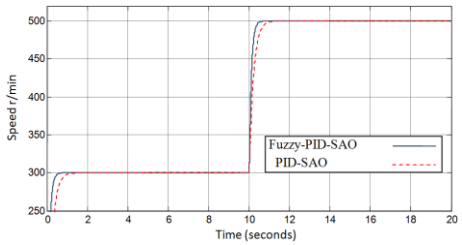

Fig. 7-a Speed responses

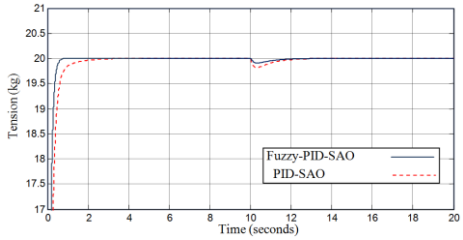

Fig. 7-b Tension (F12) responses

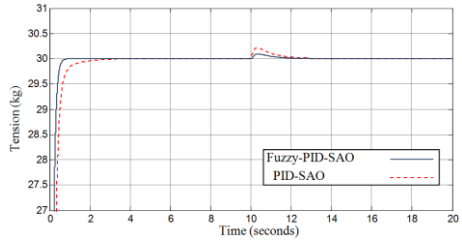

Fig. 7.c Tension (F23) responses

Fig. 7. Speed and tension responses with a sudden increase in speed

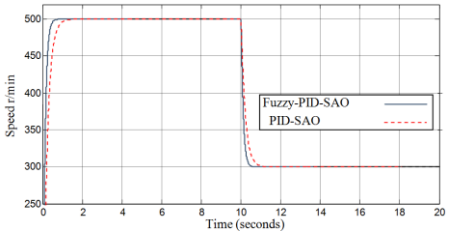

Fig. 8-a Speed responses

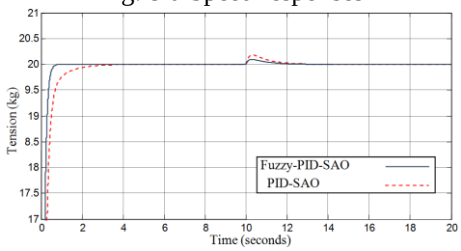

Fig. 8-b Tension (F12) responses

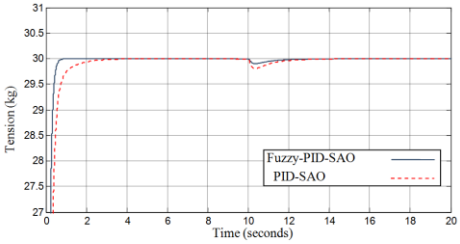

Figure (8-c) Tension (F23) responses

Fig. 8. Speed and tension responses with a sudden decrease in speed

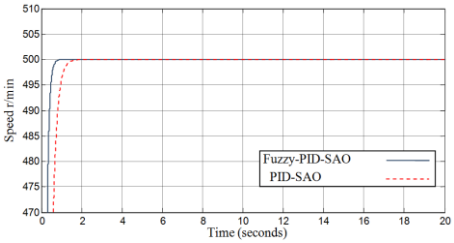

Fig. 9-a Speed responses

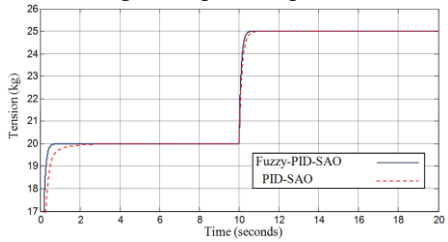

Fig. 9-b Tension (F12) responses

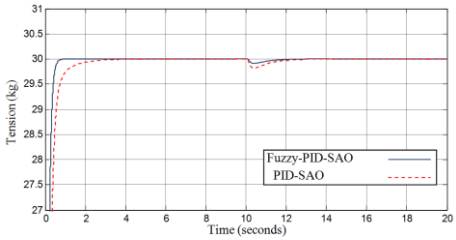

Fig. 9-c Tension (F23) responses

Fig. 9 Speed and tension responses with a sudden increase in tension (F12)

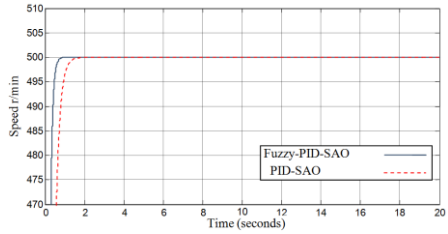

Fig. 10-a Speed responses

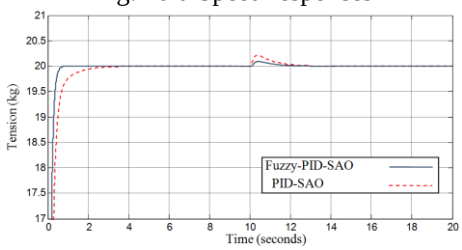

Fig. 10-b Tension (F12) responses

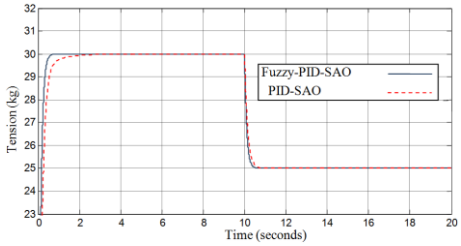

Fig. 10-c Tension (F23) responses

Fig. 10. Speed and tension responses with a sudden decrease in tension (F23)

5. Conclusion

In this paper, a robust Fuzzy-PID control using Simulated Annealing Optimization (SAO) has been firstly introduced to multi-motor drive system. A mathematical model of the three-motor drive system is deduced by considering the first motor as a main and the others as supplement motors. The proposed Fuzzy-PID-SAO controller is applied to the three-motor system using SAO technique to adjust the input and output scaling factor (SF's) by minimizing both integral of absolute of errors (IAE) and integral of time multiplied absolute of errors (ITAE) as performance measures. To test the robustness of the proposed controllers, several simulation cases are studied and presented. In all cases, the proposed controller introduces excellent, robust and faster performance compared to PID-SAO controller.

References

1. Wang, L., Ho, C. N.-M., Canales, F., Jatskevich, J.: *High-frequency modeling of the long-cable-fed induction motor drive system using TLM approach for predicting overvoltage transients.* In: IEEE Transactions on Power Electronics, Vol. 25, No.10, October 2010, p. 2653-2664.
2. Ewanchuk, J., Salmon, J., Knight, A. M.: *Performance of a high-speed motor drive system using a novel multilevel inverter topology*. In: IEEE Transactions on Industry Applications, Vol. 45, No. 5, September-October 2009, p. 1706-1714.
3. Szabat, K., Orlowska-Kowalska, T., Dybkowski, M.: *Indirect adaptive control of induction motor drive system with an elastic coupling.* In: IEEE Transactions on Industrial Electronics, Vol. 56, No. 10, October 2009, p. 4038-4042.
4. Jafarboland, M., Faiz, J.: *Modeling and designing controller of two different mechanical coupled motors for enhancement of underwater vehicles performance*. In: IET on Electric Power Applications, Vol. 4, No. 7, August 2010, p. 525-538.
5. Luo X., Liang X., Jia X., Zhang X., and Zhao K.: *Design of decoupling control system with high angle based on PV criterion*. In: Proceedings of International Symposium on Web Information Systems and Applications, May 22-24, 2009, Nanchang, China, p. 178-181.
6. Wu, Y., Deng, Z., Wang, X., Ling, X., Cao, X.: *Position sensorless control based on coordinate transformation for brushless DC motor drives.* In: IEEE Transactions on Power Electronics, Vol. 25, No. 9, September 2010, p. 2365-2371.
7. Brandao Jacobina, C., Soares de Freitas, I., Ricarte da Silva, C., Beltrao de Rossiter Correa, M., Cabral da Silva, E. R.: *Reduced switchcount six-phase AC motor drive systems without input reactor*. In: IEEE Transactions on Industrial Electronics, Vol. 55, No. 5, May 2008, p. 2024-2032.
8. Jacobina, C. B., dos Santos, E. C., de Rossiter Correa, M. B., da Silva, E. R. C.: *AC motor drives with a reduced number of switches and boost inductors*. In: IEEE Transactions on Industry Applications, Vol. 43, No. 1, January-February 2007, p. 30-39.
9. Sun, D., Shao, X., Feng, G.: *A model-free cross-coupled control for position synchronization of multi-axis motions: theory and experiments*. In: IEEE Transactions on Control Systems Technology, Vol. 15, No. 2, March 2007, p. 306-314.
10. Ren, X., Lewis, F. L., Zhang, J., Ge, S. S.: *Feedforward control based on neural networks for hard disk drives*. In: IEEE Transactions on Magnetics, Vol. 45, No. 7, July 2009, p. 3025-3030.
11. Kim, Y., Lim, M.: *Parallel optimal control for weakly coupled nonlinear systems using successive Galerkin approximation.* In: IEEE Transactions on Automatic Control, Vol. 53, No. 6, July 2008, p. 1542-1547.
12. Lin, F., Chang, C., Huang, P.: *FPGA-based adaptive backstepping sliding-mode control for linear induction motor drive*. In: IEEE Transactions on Power Electronics, Vol. 22, No. 4, July 2007, p.1222-1231.
13. Tseng, C., Chen, B.: *Robust fuzzy observer-based fuzzy control design for nonlinear discrete-time systems with persistent bounded disturbances*. In: IEEE Transactions on Fuzzy Systems, Vol. 17, No. 3, June 2009, p. 711-723.
14. Liang Z., Xingqiao L., Chong C., Guohai L., Li C.: *Simulation of Three-motor Synchronous Control System Based on BP Neural Network*. In: Control and Decision Conference, 17-19 June 2009, Zhenjiang ,China, p. 5365 – 5368.
15. Liu G., Xiao X., Teng C., Yang G., Jiang Y., Shen Y.: *Modified internal model control of induction motor variable frequency speed control system in V/F mode based on neural network generalized inverse*. In: 2010 Chinese Control and Decision Conference, May 2010, p. 3170- 3174.
16. Che Y., Sha L. K.W. Eric C.: *Variable Gain Intelligent Control of Multi-motor Synchronization System*. In: 2nd International Conference on Power Electronics Systems and Applications, 2006.
17. Fang H., Weiming T. Q. W.: *Synchronization Control Strategy of Multi-motor System Based on Profibus Network*. In: Proceedings of the IEEE International Conference on Automation and Logistics, August 18 - 21, 2007, Jinan, China.
18. Guohai L., Jinzhao Z., Tianhong P.: *Identification of Speed and Tension for Multi-motor Synchronous System based on LMN*. In: IEEE Pacific-Asia Workshop on Computational Intelligence and Industrial Application, 2008.
19. Chen C., Liu X.: *Application of Fuzzy Control in Multi-motor Tension Control System*. International Conference on Intelligent System Design and Engineering Application, 2010.
20. Jonathan, M. G., Emmanuel, C. I: *Application of Simulated Annealing Fuzzy Model Tuning to Umbilical Cord Acid-Base Interpretation*. In: IEEE Transactions on Fuzzy Systems, Vol. 7, No. 1, February 1999.
21. Gwo, C. L., Ta, P. T.: *Application of a Fuzzy Neural Network Combined With a Chaos Genetic Algorithm and Simulated Annealing to Short-Term Load Forecasting.* In: IEEE Transactions on Evolutionary

Computation, Vol. 10, No. 3, June 2006.
22. Shinn, J. H., Li, S. S., Shinn, Y. H.: *Optimizing Fuzzy Neural Networks for Tuning PID Controllers Using an Orthogonal Simulated Annealing Algorithm OSA*. In: IEEE Transactions on Fuzzy Systems, Vol. 14, No. 3, June 2006.
23. Radu-Emil, P., Radu-Codrut, D., Emil, M., Stefan, P., Mircea, R. : *Fuzzy Control Systems with Reduced Parametric Sensitivity Based on Simulated Annealing*. In: IEEE Transactions on Industrial Electronics, Vol. 59, No. 8, Aug. 2012, p. 3049-3061.
24. Gopi E. S.: *Algorithm Collections for Digital Signal Processing Applications Using Matlab.* P.O. Box 17, 3300 AA Dordrecht, Netherlands.